Independently tunable double Fano resonances in asymmetric MIM waveguide structure

Jiwei Qi, Zongqiang Chen, Jing Chen, Yudong Li, Wu Qiang, Jingjun Xu, and Qian Sun*

MOE Key Laboratory of Weak Light Nonlinear Photonics, Tianjin Key Laboratory of Photonics Material and Technology, School of Physics, Nankai University, Tianjin 300071, China

qiansun@nankai.edu.cn

Abstract: In this paper, an asymmetric plasmonic structure composed of a MIM (metal-insulator-metal) waveguide and a rectangular cavity is reported, which can support double Fano resonances originating from two different mechanisms. One of Fano resonance originates from the interference between a horizontal and a vertical resonance in the rectangular cavity. And the other is induced by the asymmetry of the plasmonic structure. Just because the double Fano resonances originate from two different mechanisms, each Fano resonance can be well tuned independently by changing the parameters of the rectangular cavity. And during the tuning process, the FOMs (figure of merit) of both the Fano resonances can keep unchanged almost with large values, both larger than 650. Such, the transmission spectra of the plasmonic structure can be well modulated to form transmission window with the position and the full width at half maximum (FWHM) can be tuned freely, which is useful for the applications in sensors, nonlinear and slow-light devices.

OCIS codes: (250.5403) Plasmonics; (240.6680) Surface plasmons; (280.4788) Optical sensing and sensors.

References and links

1. W. L. Barnes, A. Dereux, and T. W. Ebbesen, "Surface plasmon subwavelength optics," Nature **424**(6950), 824–830 (2003).
2. F. Hao, Y. Sonnefraud, P. Van Dorpe, S. A. Maier, N. J. Halas, and P. Nordlander, "Symmetry breaking in plasmonic nanocavities: subradiant LSPR sensing and a tunable Fano resonance," Nano Lett. **8**(11), 3983–3988 (2008).
3. F. Hao, P. Nordlander, Y. Sonnefraud, P. Van Dorpe, and S. A. Maier, "Tunability of subradiant dipolar and Fano-type plasmon resonances in metallic ring/disk cavities: implications for nanoscale optical sensing," ACS Nano **3**(3), 643–652 (2009).
4. J. B. Lassiter, H. Sobhani, J. A. Fan, J. Kundu, F. Capasso, P. Nordlander, and N. J. Halas, "Fano resonances in plasmonic nanoclusters: geometrical and chemical tunability," Nano Lett. **10**(8), 3184–3189 (2010).
5. J. Chen, Z. Li, S. Yue, J. Xiao, and Q. Gong, "Plasmon-induced transparency in asymmetric T-shape single slit," Nano Lett. **12**(5), 2494–2498 (2012).
6. X. Piao, S. Yu, and N. Park, "Control of Fano asymmetry in plasmon induced transparency and its application to plasmonic waveguide modulator," Opt. Express **20**(17), 18994–18999 (2012).
7. S. Zhang, K. Bao, N. J. Halas, H. Xu, and P. Nordlander, "Substrate-induced Fano resonances of a plasmonic nanocube: a route to increased-sensitivity localized surface plasmon resonance sensors revealed," Nano Lett. **11**(4), 1657–1663 (2011).
8. S. Collin, G. Vincent, R. Haïdar, N. Bardou, S. Rommeluère, and J. L. Pelouard, "Nearly perfect Fano transmission resonances through nanoslits drilled in a metallic membrane," Phys. Rev. Lett. **104**(2), 027401 (2010).
9. H. Lu, X. Liu, D. Mao, and G. Wang, "Plasmonic nanosensor based on Fano resonance in waveguide-coupled resonators," Opt. Lett. **37**(18), 3780–3782 (2012).
10. H. Lu, X. Liu, D. Mao, Y. Gong, and G. Wang, "Induced transparency in nanoscale plasmonic resonator systems," Opt. Lett. **36**(16), 3233–3235 (2011).
11. J. Chen, Z. Li, J. Li, and Q. Gong, "Compact and high-resolution plasmonic wavelength demultiplexers based on Fano interference," Opt. Express **19**(10), 9976–9985 (2011).

#210137 - $15.00 USD Received 14 Apr 2014; revised 22 May 2014; accepted 26 May 2014; published 6 Jun 2014

12. J. Chen, C. Wang, R. Zhang, and J. Xiao, "Multiple plasmon-induced transparencies in coupled-resonator systems," Opt. Lett. **37**(24), 5133–5135 (2012).
13. Z. Yang, Q. Wu, and H. Lin, "Tunable two types of Fano resonances in metal-dielectric core-shell nanoparticle clusters," Appl. Phys. Lett. **103**(11), 111115 (2013).
14. J. B. Lassiter, H. Sobhani, M. W. Knight, W. S. Mielczarek, P. Nordlander, and N. J. Halas, "Designing and deconstructing the Fano lineshape in plasmonic nanoclusters," Nano Lett. **12**(2), 1058–1062 (2012).
15. B. Luk'yanchuk, N. I. Zheludev, S. A. Maier, N. J. Halas, P. Nordlander, H. Giessen, and C. T. Chong, "The Fano resonance in plasmonic nanostructures and metamaterials," Nat. Mater. **9**(9), 707–715 (2010).
16. V. A. Fedotov, M. Rose, S. L. Prosvirnin, N. Papasimakis, and N. I. Zheludev, "Sharp trapped-mode resonances in planar metamaterials with a broken structural symmetry," Phys. Rev. Lett. **99**(14), 147401 (2007).
17. C. Wu, A. B. Khanikaev, and G. Shvets, "Broadband slow light metamaterial based on a double-continuum Fano resonance," Phys. Rev. Lett. **106**(10), 107403 (2011).
18. A. Artar, A. A. Yanik, and H. Altug, "Multispectral plasmon induced transparency in coupled meta-atoms," Nano Lett. **11**(4), 1685–1689 (2011).
19. A. Artar, A. A. Yanik, and H. Altug, "Directional double Fano resonances in plasmonic hetero-oligomers," Nano Lett. **11**(9), 3694–3700 (2011).
20. S. D. Liu, Z. Yang, R. P. Liu, and X. Y. Li, "Multiple Fano resonances in plasmonic heptamer clusters composed of split nanorings," ACS Nano **6**(7), 6260–6271 (2012).
21. J. Wang, C. Fan, J. He, P. Ding, E. Liang, and Q. Xue, "Double Fano resonances due to interplay of electric and magnetic plasmon modes in planar plasmonic structure with high sensing sensitivity," Opt. Express **21**(2), 2236–2244 (2013).
22. D. Wang, X. Yu, and Q. Yu, "Tuning multiple Fano and plasmon resonances in rectangle grid quasi-3D plasmonic-photonic nanostructures," Appl. Phys. Lett. **103**(5), 053117 (2013).
23. Z. Han, E. Forsberg, and S. He, "Surface plasmon Bragg gratings formed in metal-insulator-metal waveguides," IEEE Photon. Technol. Lett. **19**(2), 91–93 (2007).
24. Z. Chen, J. Qi, J. Chen, Y. Li, Z. Hao, W. Lu, J. Xu, and Q. Sun, "Fano resonance based on multimode interference in symmetric plasmonic structures and its applications in plasmonic nanosensors," Chin. Phys. Lett. **30**(5), 057301 (2013).
25. X. Piao, S. Yu, S. Koo, K. Lee, and N. Park, "Fano-type spectral asymmetry and its control for plasmonic metal-insulator-metal stub structures," Opt. Express **19**(11), 10907–10912 (2011).
26. J. Becker, A. Trügler, A. Jakab, U. Hohenester, and C. Sönnichsen, "The optimal aspect ratio of gold nanorods for plasmonic bio-sensing," Plasmonics **5**(2), 161–167 (2010).
27. Y. Kou and X. F. Chen, "Multimode interference demultiplexers and splitters in metal-insulator-metal waveguides," Opt. Express **19**(7), 6042–6047 (2011).

1. Introduction

The Fano resonance arises from the coherent coupling and interference between a discrete state and a continuous state. Recently, the Fano resonance in nanoplasmonic structure aroused more attention, because surface plasmon polaritons (SPPs) can overcome the diffraction limit and confine light in sub-wavelength dimensions [1]. Many plasmonic structures have been designed to achieve the Fano resonance. Usually, a common way to obtain the Fano resonance is by using symmetry-breaking plasmonic structures, such as the broken symmetry in ring or disk cavities [2, 3], asymmetric plasmonic nanoclusters [4], asymmetric T-shape single slit [5], asymmetric stub pair in Metal-insulator-metal (MIM) waveguide [6], and plasmonic nanocube in an adjacent semi-infinite dielectric [7]. Additionally, the Fano resonance also can be obtained in the symmetric plasmonic structures, include utilizing freestanding metallic gratings with narrow slits [8], cavity-cavity interference [9, 10], strong couplings of coupled-resonator systems [11, 12], the coupling of plasmonic nanoclusters [13, 14], Due to the physics origin as an interference phenomenon and the unique line shape of the Fano resonance, the devices based on the Fano resonance have shown great sensitivity and large figure of merit (FOM), which can be used in sensors, lasing, switching, nonlinear and slow-light devices [15].

For some specific plasmonic structures, multiple Fano resonances can be obtained. Due to the advantage for enhanced bio-chemical sensing, spectroscopy, and multicolor nonlinear processes, the multiple Fano resonances become more important and have gained much attention [16–22]. Fedotov et al. [16] certificated that the planar metamaterials composed of asymmetrically split rings exhibit strong high-Q resonances and provide for double-Fano resonances. Wu et al. [17] proposed broadband slow light metamaterial based on double Fano resonances. Artar et al. [18, 19] showed double Fano resonances and multispectral plasmon Iinduced transparency (PIT) in plasmonic oligomers. Liu et al. [20] achieved multiple Fano

#210137 - $15.00 USD Received 14 Apr 2014; revised 22 May 2014; accepted 26 May 2014; published 6 Jun 2014

resonances in plasmonic heptamer clusters composed of split nanorings. J. Wang et al. [21] reported a planar plasmonic structure to obtain double Fano resonances originated from interplay of electric and magnetic plasmon modes. D. Wang [22] realized tuning multiple Fano and plasmon resonances in plasmonic-photonic nanostructures. For many applications, tunability of the Fano resonances is very important. However, because the multiple Fano resonances are caused by the collective behavior of the total plasmonic systems, it is difficult to get an independent and precise tailoring of the multiple Fano resonances.

In this paper, independently tunable double Fano resonances are realized in asymmetric plasmonic structure. Symmetry-breaking is induced by embedding a rectangular cavity asymmetrically into a plasmonic MIM waveguide. In our proposed asymmetric plasmonic structure, the double Fano resonances originate from two different mechanisms, one originates from the interference between a horizontal and a vertical resonance in the rectangular cavity, and the other originates from the asymmetry of the MIM waveguide plasmonic structure. Because of the different mechanisms of the two Fano resonances, the double Fano resonances can be tuned independently through changing the length and height of the rectangular cavity, respectively. In the tuning process, the FOMs of the double Fano resonances unchanged almost and keep high value, both larger than 650. Attributed to the large FOM and independent tunabilities of the double Fano resonances, the transmission spectra can be well tailored. The devices based on our tunable double Fano resonances waveguide structure can be used in filters, enhanced bio-chemical sensors, switches and modulator of high density nano-photonic integrated circuits devices with excellent performance.

2. Sturctures descriptions

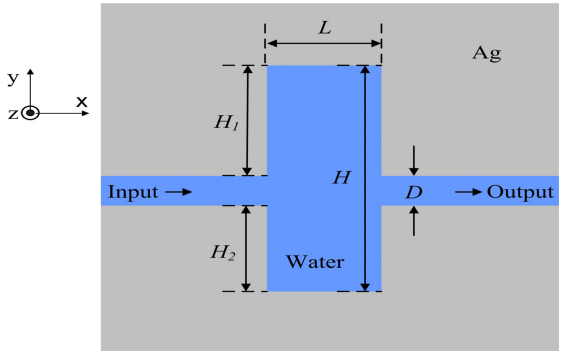

Fig. 1. Schematic diagram of the asymmetric plasmonic structure composed of a MIM waveguide and a rectangular cavity.

Figure 1 shows the two-dimensional geometry of the asymmetric plasmonic structure composed of a MIM waveguide and a rectangular cavity. The length and height of the rectangular cavity are denoted as L and H, respectively. Symmetry-breaking is induced by changing the relative positions between the axes of the MIM waveguide and the rectangular cavity in y direction. $\Delta H = H_1\text{-}H_2$, as shown in Fig. 1, is used to describe the symmetry-breaking. The width of the waveguide is D. Taking into account the application in biotechnology, the insulators in the waveguide and cavity are chosen to be water ($n_d = 1.33$). The metal is sliver, whose frequency-dependent complex relative permittivity is characterized by the Drude model:

$$\varepsilon_m(\omega) = \varepsilon_\infty - \omega_p^2 / \omega(\omega + i\gamma). \quad (1)$$

Here, ε_∞ is the dielectric constant at the infinite frequency, γ is the electron collision frequency, ω_p is bulk plasma frequency, and ω is the angular frequency of incident light. The

#210137 - $15.00 USD Received 14 Apr 2014; revised 22 May 2014; accepted 26 May 2014; published 6 Jun 2014

parameters are ε_∞ = 3.7, ω_p = 9.1 eV, γ = 0.018 eV [23]. In order to excite the SPPs, the input light is set to be transverse magnetic (TM) plane wave.

The transmittance of the plasmonic structure is researched by using commercial software (COMSOL Multiphysics) of the finite-element analysis method (FEM). The transmittance is defined as $T = |\mathbf{H}_{zout}|^2 / |\mathbf{H}_{zin}|^2$, where $|\mathbf{H}_{zin}|$ and $|\mathbf{H}_{zout}|$ are the input and output amplitudes of magnetic field, respectively.

3. Simulation results and discussions

Figure 2 shows the different mechanisms of the double Fano resonances. The interferences between the eigenmodes in the rectangular cavity are the origins of Fano resonances. The eigenmodes of a rectangular cavity are researched by using COMSOL Multiphysics. Because the input light is set to be transverse magnetic (TM) plane wave, the resonant modes can be classified using $TM_{m,n}$, m, n are integers and indicate the x- and y-directional resonant orders, respectively. When the parameters of the structure are L = 220 nm, H = 760 nm, ΔH = 0, and D = 50 nm, the transmittance of the plasmonic structure is shown as the black line in Fig. 2(a). Here the structure is symmetric. Single Fano profile peak presents at about 735 nm, which originates from the interference of the narrow $TM_{1,0}$ mode at about 735 nm (corresponding to the x direction resonance in the rectangular cavity) with a broad $TM_{0,2}$ mode at about 1082 nm (corresponding to the y direction resonance in the rectangular cavity). The distribution of the normalized z-direction magnetic field $\mathbf{H}_z$ of the eigenmodes, the $TM_{1,0}$ mode and $TM_{0,2}$ mode, are shown in Figs. 2(c) and (e), respectively. This kind of Fano resonance has been certificated in our previous work [24] and is called FR 1 in the following.

When the symmetry-breaking was induced in our plasmonic structure, two Fano resonances occurred simultaneously. Figure 2(a) shows the comparing transmittance of the plasmonic structure with different spatial asymmetry. The transmittance of the plasmonic structure with L = 220 nm, H = 760 nm, ΔH = 10 nm, and D = 50 nm is shown as red line in Fig. 2(a). Another Fano resonance peak presented at about 783nm which is caused by symmetry-breaking of the MIM waveguide plasmonic structure, similar with the results in the reference 5, and is called FR 2 in the following. When the symmetry-breaking of the MIM waveguide plasmonic structure was induced, a narrow $TM_{0,3}$ mode at about 783 nm in the rectangular cavity is excited, which is apparent in symmetrical MIM waveguide plasmonic structure. The distribution of the normalized z-direction magnetic field $\mathbf{H}_z$ of the eigenmode, $TM_{0,3}$ mode, is shown in Fig. 2(d). The FR 2 originates from the interference between the narrow $TM_{0,3}$ mode and the broad $TM_{0,2}$ mode. And with the spatial asymmetry increasing, for an example that ΔH changes from 10 nm to 20 nm, the transmission of FR 2 becomes larger, from about 40% to about 70%. It is noteworthy that with the increase of ΔH from 0 nm to 20 nm, the position and the intensity of FR 1 remains unchanged almost, as shown in Fig. 2 (a). This implies that $TM_{1,0}$ mode $TM_{0,2}$ mode remain unchanged almost in the increasing process of the spatial asymmetry. And with the increase of ΔH from 0 nm to 20 nm, a little platform appears at about 729 nm, which is caused by the symmetry-breaking of the MIM waveguide plasmonic structure. Another noteworthy feature is that the Fano line-shapes of FR 1 and FR 2 are different with each other, the 'direction' of Fano asymmetry is reversed between FR 1 and FR 2. This phenomenon attributes to the different phase shifts of the three eigenmodes. The phase shift is defined as the phase difference between the input position and the output position, which can be estimated according Figs. 2(c)–2(e). As shown in Figs. 2(c)–2(e), the phase shift of $TM_{1,0}$ mode (narrow state of FR 1) is about π, while the phase shifts of $TM_{0,3}$ mode (narrow state of FR 1) and $TM_{0,2}$ mode (broad state of FR 1 and FR 2) both are about 0. The reversed phase shifts of $TM_{1,0}$ mode with $TM_{0,3}$ mode and $TM_{0,2}$ mode result in the reversed 'direction' of Fano asymmetry [25]. The reversed 'direction' of Fano asymmetry can support the formation of the transmission window which is very useful for applications in nonlinear and slow-light devices. And this result also indicates that the 'direction' of Fano asymmetry can be tuned by changing the relative phase shift between the narrow state and the broad state. Figure 2(b) depicts the

#210137 - $15.00 USD Received 14 Apr 2014; revised 22 May 2014; accepted 26 May 2014; published 6 Jun 2014

distribution of normalized magnetic field $\mathbf{H}_z$ at the wavelengths 735 nm and 783 nm, respectively, with the structure parameters of L = 220 nm, H = 760 nm, D = 50 nm and ΔH = 20 nm. The distribution $\mathbf{H}_z$ at the wavelength 735 nm shows the interference between the narrow $TM_{1,0}$ mode and the broad $TM_{0,2}$ mode, and the distribution $\mathbf{H}_z$ at the wavelength 783 nm shows the interference between the narrow $TM_{0,3}$ mode and the broad $TM_{0,2}$ mode. As shown in Fig. 2, double reversed Fano resonances originated from two different mechanisms, were realized simultaneously in one MIM waveguide structure.

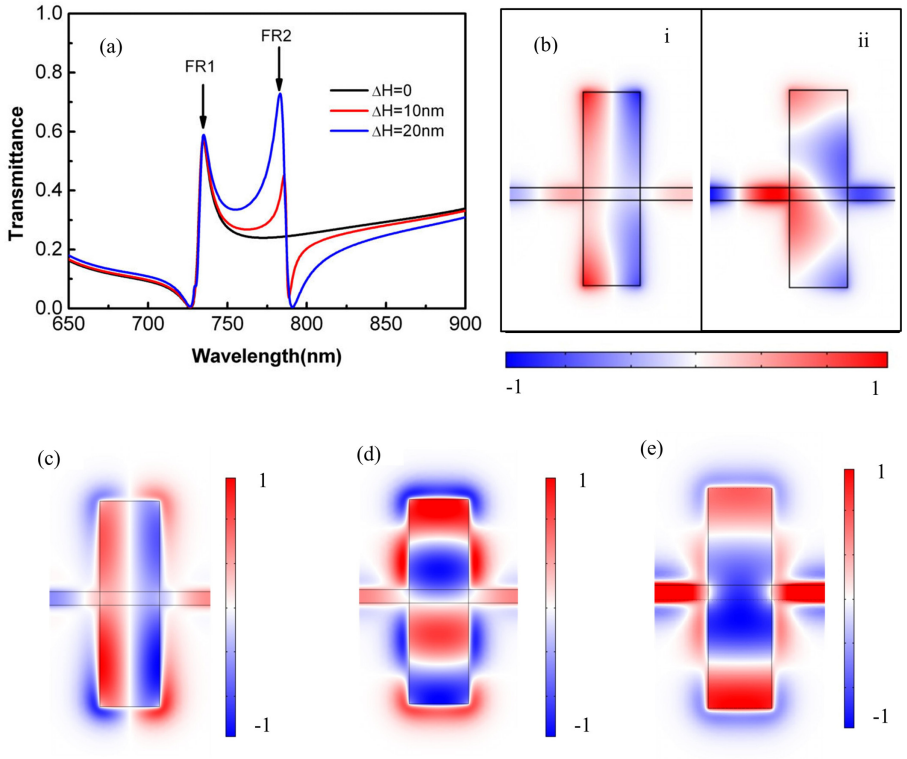

Fig. 2. (a)The transmission spectra of the plasmonic structure with L = 220 nm, H = 760 nm, D = 50 nm and ΔH = 0 (black line); ΔH = 10 nm (red line); ΔH = 20 nm (blue line). (b)The normalized z-direction magnetic field $(\mathbf{H})_z$ in the structure with L = 220 nm, H = 760 nm, D = 50 nm and ΔH = 20 nm: (i) FR 1 at 735 nm, (ii) FR 2 at 783 nm. (c)-(e) The distribution of the normalized z-direction magnetic field $(\mathbf{H})_z$ of the eigenmodes $TM_{1,0}$ mode at 735 nm,$TM_{0,3}$ mode at 783 nm and $TM_{0,2}$ mode at 1082 nm respectively in the rectangular cavity with L = 220 nm, H = 760 nm.

FOM is a key parameter for Fano resonance. The Fano resonance detects rather a relative intensity change $dI(\lambda)/dn(\lambda)$ at fixed wavelength λ_0. A FOM is defined as [26]:

$$\mathrm{FOM} = \max\left|\frac{dI(\lambda)/dn(\lambda)}{I(\lambda)}\right|. \qquad (2)$$

$dI(\lambda)/dn(\lambda)$ is the relative intensity change at fixed wavelength induced by a refractive index change dn. $I(\lambda_0)$ corresponds to the intensity where FOM reaches a maximum value. Figure 3(a) shows the transmission spectra for different refractive indexes of the insulators in the waveguide and cavity with the structure parameters of L = 220 nm, H = 760 nm, D = 50 nm and ΔH = 20 nm. The insert shows the peak positions of FR 1 and FR 2 change with refractive indexes of the insulators in the waveguide and cavity (n). With the increasing of n from 1.33 to

#210137 - $15.00 USD Received 14 Apr 2014; revised 22 May 2014; accepted 26 May 2014; published 6 Jun 2014

1.35, the peaks of FR 1 and FR 2 are both red shift, the peaks of FR 1 red shifts from about 735 nm to 746 nm and the peaks of FR 2 red shifts from about 783 nm to 795 nm. This agrees with the dispersion relation of MIM waveguide [27]. Figure 3(b) shows the FOM curve and the corresponded transmission spectrum with the structure parameters of L = 220 nm, H = 760 nm, D = 50 nm, ΔH = 20 nm and n = 1.33. As shown in Fig. 3(b), the maxes of FR 1 and FR 2 are about 650 and 850 respectively. FR 2 is more sensitive than FR 1. And there is a steep change of FOM at about 729 nm, which is induced by the little platform located at 729 nm.

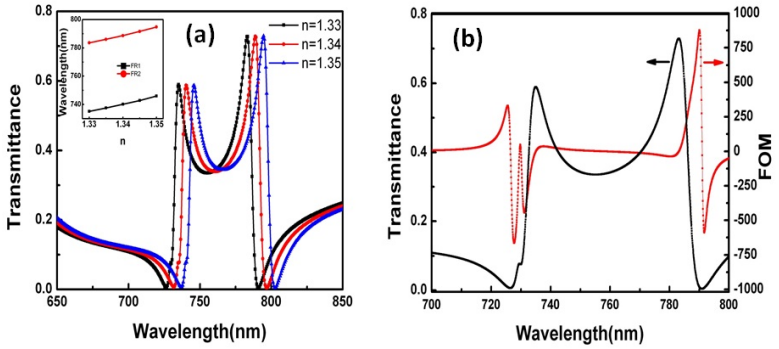

Fig. 3. (a) The transmission spectra of the plasmonic structure with L = 220 nm, H = 760 nm, D = 50 nm, ΔH = 20 nm, and different refractive indexes of the insulators in the waveguide and cavity, n = 1.33 (black line), n = 1.34 (red line), n = 1.35 (blue line). The insert: The peak positions of FR 1 (black line) and FR 2 (red line) change with the refractive indexes of the insulators in the waveguide and cavity. (b) The FOM curve and the corresponded transmission spectrum with the structure parameters of L = 220 nm, H = 760 nm, D = 50 nm, ΔH = 20 nm, n = 1.33.

Just because the narrow states of FR 1 and FR 2 correspond to the x direction resonance and y direction resonance in the rectangular cavity respectively, the two Fano resonances, FR 1 and FR 2, can be tuned independently by changing the length (L) and the height (H) of the rectangular cavity. According to the dispersion relation of MIM waveguide [27], the transmission peak of $TM_{1,0}$ mode red shifts with the increasing of L and is unsensitive to H; the transmission peaks of $TM_{0,2}$ mode and $TM_{0,3}$ mode red shift with the increasing of H and is unsensitive to L. The influence of the structure parameters on the transmission spectrum profile is studied in detail and the results are shown in Fig. 4. Figure 4(a) depicts that the position of FR 1 can be tuned by the length of the rectangular cavity (L). As shown in Fig. 4(a), with L increasing from 215 nm to 235 nm, the position of the FR 1 changes from about 720 nm to about 775 nm. At the same time, the change in FR 2 position is small, only about 8 nm. Figure 4(b) depicts that the position of the FR 2 can be tuned by the height of the rectangular cavity (H). As shown in Fig. 4(b), with H increasing from 730 nm to 780 nm, the position of the FR 2 changes from 756 nm to 806 nm, and simultaneously, almost no change in the position of FR 1 (<2 nm). Additionally, the decreases of FR 1 and FR 2 peak intensities imply the red shift of $TM_{0,2}$ mode with the increasing of H. Thus, due to the independent tunabilities of the narrow states of FR 1 and FR 2, $TM_{1,0}$ mode and $TM_{0,3}$ mode, the two Fano resonances can be tuned independently. Our results agree with the dispersion relation of MIM waveguide. And as shown in Figs. 4(c) and 4(d), with the change of the length (L) and the height (H) of the rectangular cavity, the FOM of FR 1 and FR 2 change slightly, no more than 6%. This means that the FOMs of the double Fano resonances keep high value in the tuning process.

#210137 - $15.00 USD Received 14 Apr 2014; revised 22 May 2014; accepted 26 May 2014; published 6 Jun 2014

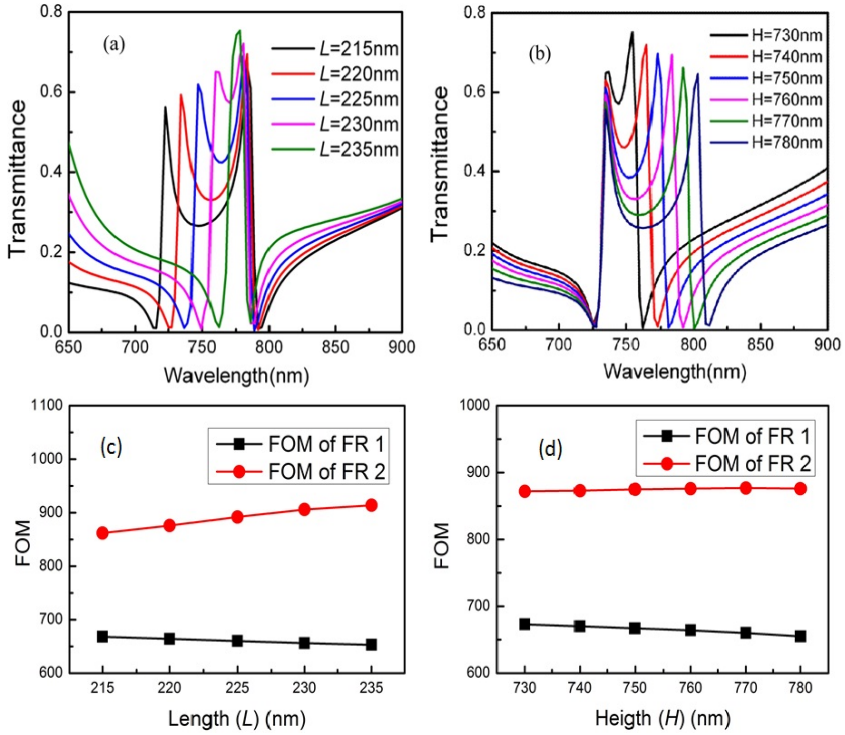

Fig. 4. The dependence of tansmission on the structure parameters. (a) Different L with fixed H = 760 nm, ΔH = 20 nm and D = 50 nm; (b) different H with fixed L = 760 nm, ΔH = 20 nm and D = 50 nm. (c) and (d) The change curves of FOM of FR 1 (black line) and FR 2 (red line) with the change of the structure parameters, L and H respectively.

Attribute to the reversed 'direction' of Fano asymmetry, the large FOMs and the independent tunability of FR 1 and FR 2, the transmission spectra of the double Fano resonances structure can be well tailored and transmission window can be constructed with the position and the full width at half maximum (FWHM) can be adjusted freely. A rectangular-like line-shape transmission window of the proposed structure is shown as black line in Fig. 4, with the parameters of the structure to be L = 220 nm, H = 720 nm, ΔH = 15 nm, and D = 50 nm. And because the position of the two Fano resonances can be tuned by the length and the height of the rectangular cavity independently, the center and the width of the rectangular-like line-shape can be well tuned, respectively. As shown in Fig. 5, the rectangular-like line-shape transmittance (black line) can be compressed to a narrow Lorentzian-like line-shape transmittance (red line) with the FWHM of about 7nm by changing the parameters of the structure to be L = 222 nm, H = 715 nm, ΔH = 15 nm, and D = 50 nm. The small FWHM of the narrow Lorentzian-like line-shape transmittance window also attributes to the large FOMs of FR 1 and FR 2. This kind of transmission window, whose position and FWHM can be adjusted freely, can be used in filters, enhanced bio-chemical sensors, nonlinear and slow-light devices.

#210137 - $15.00 USD Received 14 Apr 2014; revised 22 May 2014; accepted 26 May 2014; published 6 Jun 2014

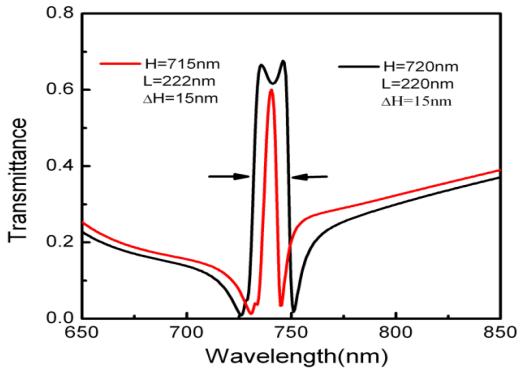

Fig. 5. Rectangular-like line-shape of the transmission spectrum in the plasmonic structure with L = 220 nm, H = 720 nm, D = 50 nm, and ΔH = 15 nm (black line); L = 222 nm, H = 715 nm, D = 50 nm and ΔH = 15 nm (red line).

4. Conclusions

In summary, we report an asymmetric plasmonic structure composed of a MIM waveguide and a rectangular cavity with their axes having a deviation. It can support double Fano resonances originating from two different mechanisms. One mechanism originates from the interference between a horizontal and a vertical resonance in a rectangular cavity, and the other originates from the symmetry-breaking of the plasmonic structure. The double Fano resonances can be well tuned independently by changing the length and height of the rectangular cavity, respectively, and the FOMs of the double Fano resonances keep almost unchanged, both larger than 650. By tuning the positions of the two Fano resonances, the transmission spectra can be well tailored. Rectangular-like line-shape and narrow Lorentzian-like line-shape transmission windows can be constructed. Benefited from the reversed 'direction' of Fano asymmetry,the large FOM, independent tunabilities and the compactness, the double Fano resonances can be used in filters, enhanced bio-chemical sensors, switches and modulator of high density nano-photonic integrated circuits devices with excellent performance.

Acknowledgments

This work is supported by National Natural Science Foundation of China (61178004), Tianjin Natural Science Foundation (12JCQNJC01100, 13JCQNJC01700), Research Fund for the Doctoral Program of Higher Education of China (NO. 20110031120005), Program for Changjiang Scholars and Innovative Research Team in Nankai University. 111 Project under Grant No B07013, and Fundamental Research Funds for the Central Universities.

#210137 - $15.00 USD Received 14 Apr 2014; revised 22 May 2014; accepted 26 May 2014; published 6 Jun 2014